

## Self-Repairing Photosensitized Electron Transfer from Thiones to Methyl Viologen in Aqueous Media

Maksudul M. Alam and Osamu Ito\*

*Institute for Chemical Reaction Science, Tohoku University, Katahira, Aoba-ku, Sendai 980-8577, Japan*

*Received: December 4, 1998*

Reversible formation of the persistent methyl viologen radical cation ( $MV^{\bullet+}$ ) was observed by the steady-state photoillumination of thiones in the presence of  $MV^{2+}$  in deaerated aqueous solution. Formation yield and lifetime of  $MV^{\bullet+}$  are favorable at a pH higher than 3.00. By laser flash photolysis, it was observed that fast electron transfer occurs from triplet states of thiones ( $^3PT^*$ ) to  $MV^{2+}$ , yielding the radical cation of thiones ( $PT^{\bullet+}$ ) and  $MV^{\bullet+}$ . The initial rapid decay of  $MV^{\bullet+}$  is attributed to back electron transfer from  $MV^{\bullet+}$  to  $PT^{\bullet+}$ . On the other hand, the slow decay part of  $MV^{\bullet+}$  can be attributed to endothermic electron transfer from  $MV^{\bullet+}$  to disulfide, which is formed by the coupling of the thio radical produced after deprotonation of  $PT^{\bullet+}$ . The ratio of slow decay component and fast decay component of  $MV^{\bullet+}$  in the short time scale is a good measure of the yields of persistent  $MV^{\bullet+}$  with changing thiones and pH. A cyclic mechanism interpreting reversible electron transfer was proposed in which thiones act as self-repairing photosensitizers.

### Introduction

Numerous photochemical investigations have long been made on the reduction of methyl viologen dication ( $MV^{2+}$ ) as a model system for the photogeneration of electric and chemical energy.<sup>1–7</sup> Various photoexcitable substances have been used as sensitizers for the production of the long-lived methyl viologen radical cation ( $MV^{\bullet+}$ ) in the presence of the appropriate catalyst and various substrates.<sup>8–10</sup> In general, addition of an excess of a “sacrificial” electron donor is necessary to repair the photooxidized sensitizers, resulting in the whole process becoming cyclic with respect to both photosensitizer and  $MV^{2+}$ .<sup>11–13</sup> The net reaction is thus the sensitizer-catalyzed photoreduction of  $MV^{2+}$  by the sacrificial electron donor.

The necessity of a sacrificial electron donor for the photo-production of the long-lived  $MV^{\bullet+}$  is a demerit to keep the reaction system reproducible for a long time. Thus, it is necessary to search for efficient sensitizers that are able to generate the long-lived  $MV^{\bullet+}$  without a sacrificial electron donor, making the processes cyclic including photosensitizer.

In the previous study, we revealed that the excited triplet states of thiones with N atoms such as pyridine-2(1*H*)-thione (2-PyT), pyridine-4(1*H*)-thione (4-PyT), and 6*H*-purine-6-thione (PuT) have high electron-donor ability by means of laser flash photolysis.<sup>14,15</sup> In the present paper, we applied these thiones as efficient photosensitizers for the production of the long-lived  $MV^{\bullet+}$  without a sacrificial electron donor. We present the results of a detailed mechanistic study of the photoreduction of  $MV^{2+}$  by the triplet states ( $^3PT^*$ ) of these pyridinthiones and purinthione (PT) for the production of the long-lived  $MV^{\bullet+}$  in aqueous media. The effect of pH on the persistency and the formation quantum yield of  $MV^{\bullet+}$  has been revealed by means of laser flash and steady-state photolysis methods. Finally, we found that PT's are effective photosensitizers with self-repairing ability.

### Experimental Section

**Materials.** Commercially available pyridine and purine thiones (PT) and dipyridine disulfides (DPDS) were purchased

from Aldrich Chemical Co. as the best purity grades. 1,1'-Dimethyl-4,4'-bipyridinium ion (methyl viologen,  $MV^{2+}$ ) was obtained as the trihydrated chloride salt (Sigma Chemical Co.). The buffer solutions pH 1.68, 4.01, 7.00, and 9.18 (Kanto Chemical Co.) were used for the transient absorption measurements.

**Steady Photolysis.** The steady photolysis of PT's with  $MV^{2+}$  in Ar-saturated buffer solutions with light of wavelength longer than 330 nm from Xe–Hg lamp (150 W) was performed and the formation of  $MV^{\bullet+}$  was checked time to time by observing the UV/vis spectrum of the photolyzed solution. To separate the reaction intermediates, reaction systems including  $MV^{\bullet+}$  were quenched by adding  $O_2$ ; the neutral products were extracted with ether and separated by TLC (Merk; Kiesegel 60F and benzene as an eluent). The products were confirmed by comparing with the characteristic spectra of authentic samples.

**Transient Absorption Measurements.** The nanosecond laser flash photolysis apparatus was a standard design with Nd:YAG laser (fwhm 6 ns).<sup>14,15</sup> The solutions were photolyzed with THG light (355 nm). The time profiles were followed by a photomultiplier tube (PMT) as a detector.<sup>16a,b</sup> The deaerated and  $O_2$ -saturated sample solutions for photolysis were obtained by Ar and  $O_2$  gas bubbling, respectively, in a rectangular quartz cell with a 10 mm optical path at 23 °C.

Absorption spectra of the radical cations of thiones were measured by  $\gamma$  irradiation in frozen glassy butyl chloride at 77 K.

**MO Calculations.** The SOMO energies of the triplet states of thiones were calculated by the unrestricted open-shell Hartree–Fock (UOHF) method on the geometries optimized at the MNDO/CI level using the MOPAC program package.<sup>17</sup> The LUMO energies of the corresponding disulfides were calculated by the restricted Hartree–Fock (RHF) method.<sup>17</sup>

### Results and Discussion

**Steady-State Absorption Spectra.** Figure 1A shows the steady absorption spectra of 2-PyT (0.2 mM) in aqueous buffer

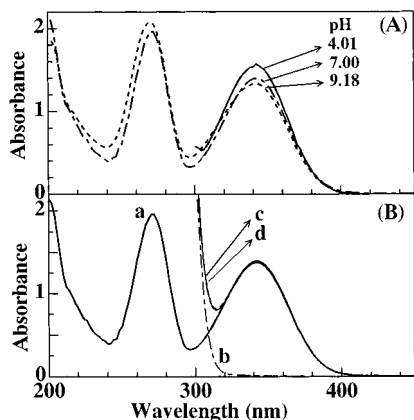


**Figure 1.** (A) Steady-state absorption spectra of 2-PyT (0.2 mM) in aqueous buffer solutions with optical path length 1.0 cm. The spectrum shorter than 300 nm in pH 4.01 was not observed due to the absorbance of buffer solution at pH 4.01. (B) spectra of (a) 2-PyT (0.2 mM), (b)  $MV^{2+}$  (3.0 mM), and (c) their mixture and (d) the simulated spectrum in aqueous solution at pH 7.00.

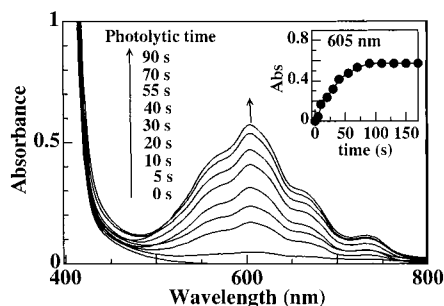


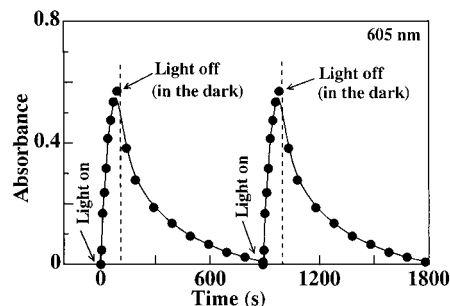
**Figure 2.** Absorption spectral changes observed by steady photolysis of 2-PyT (1.0 mM) in the presence of  $MV^{2+}$  (3.0 mM) with light (>330 nm) in Ar-saturated aqueous solution at pH 7.00. The inset shows the rise plot of  $MV^{2+}$  at 605 nm.

solutions at pH 4.01, 7.00, and 9.18. By changing the pH in the range 1.68–9.18, no significant change in the steady-state absorption spectra of 2-PyT was observed. In addition, the absorption spectrum of the mixture of 2-PyT and  $MV^{2+}$  is shown to be equal to the simulated one by adding each solution of 2-PyT and  $MV^{2+}$  (Figure 1B). No evidence for ground-state interaction was found under the experimental conditions used. Similar results were observed for 4-PyT and PuT.

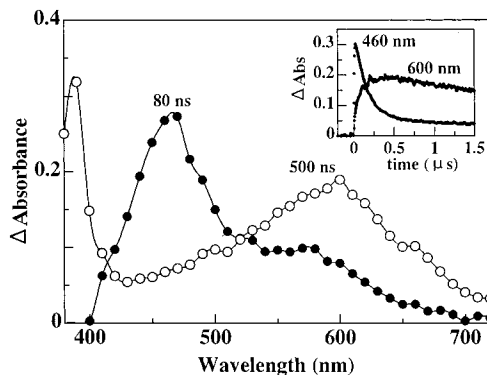
**Steady-State Photolysis. Reversibility of Photoreduction Reaction.** The spectral changes observed by steady-light (>330 nm) illumination of 2-PyT (1.0 mM) in the presence of  $MV^{2+}$  (3.0 mM) in aqueous buffer solution at pH 7.00 are shown in Figure 2. The new absorption band appearing at 605 nm is attributed to the methyl viologen radical cation ( $MV^{\bullet+}$ ).<sup>6,13,18,19</sup> The absorption intensity of  $MV^{\bullet+}$  increases with the time of the steady-light illumination and reaches a maximum concentration at ca. 1.5 min (inset of Figure 2). The inset of Figure 2 also shows that the maximal concentration of  $MV^{\bullet+}$  almost remains the same during illumination for a long time.

Figure 3 shows that  $MV^{\bullet+}$  decays slowly after switching-off the light source, indicating that  $MV^{\bullet+}$  is reoxidized to  $MV^{2+}$  in the dark. After the complete disappearance,  $MV^{\bullet+}$  was regenerated by switching-on the light again, indicating that the reproducibility of the phenomenon; i.e., the reversible photoredox process takes place.<sup>7a,11,13</sup>

Such a reversible photoredox process was observed in buffer solutions at pH 9.18 and 4.01 and also for 4-PyT and PuT. At pH 1.68, on the other hand, no spectral change due to the



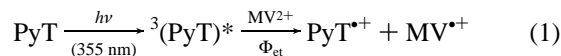
**Figure 3.** Plot of absorption intensity of  $MV^{2+}$  at 605 nm vs time under steady illumination and in the dark of the same system as in Figure 2.



**Figure 4.** Transient absorption spectra observed by laser photolysis of 2-PyT (0.2 mM) in the presence of  $MV^{2+}$  (0.8 mM) with 355 nm light in Ar-saturated aqueous solution at pH 7.00. The inset shows time profiles of absorption bands at 460 and 600 nm.

formation of the long-lived  $MV^{\bullet+}$  was observed by the steady-light illumination of all thiones (2-PyT, 4-PyT, and PuT) with  $MV^{2+}$ .

**Transient Absorption Spectra.** The transient absorption measurements were performed by laser photolysis to understand the role of the triplet states of thiones and the mechanism of the photoredox reaction for the generation of the long-lived  $MV^{\bullet+}$  in aqueous solutions. The transient absorption spectra observed by laser photolysis of 2-PyT (0.2 mM) with 355 nm light in the presence of  $MV^{2+}$  (0.8 mM) in Ar-saturated aqueous solution (pH 7.00) are shown in Figure 4. An absorption peak at 460 nm, which is observed immediately after the nanosecond laser pulse, is attributed to the triplet–triplet absorption band of 2-PyT [ $^3(2\text{-PyT})^*$ ], as assigned in our previous study.<sup>15</sup> The decay of  $^3(2\text{-PyT})^*$  was accelerated in the presence of  $MV^{2+}$ . After the decay of  $^3(2\text{-PyT})^*$ , new absorption bands of  $MV^{\bullet+}$  appeared at 390 and 600 nm.<sup>6,13,18,19</sup> The decay rate of  $^3(2\text{-PyT})^*$  at 460 nm seems to be in good agreement with the rise rate of  $MV^{\bullet+}$  at 600 nm (inset in Figure 4), indicating that  $MV^{\bullet+}$  is formed due to electron transfer from  $^3(2\text{-PyT})^*$  to  $MV^{2+}$  at pH 7.00 as in eq 1.<sup>7a,11,14,15</sup>



A similar behavior was observed at pH 4.01 and 9.18. With the decay of  $^3(4\text{-PyT})^*$  at 430 nm [or  $^3(\text{PuT})^*$  at 475 nm],<sup>14,15</sup> the rise of  $MV^{\bullet+}$  was observed by the laser photolysis of 4-PyT (or PuT) in the presence of  $MV^{2+}$  with 355 nm light in Ar-saturated buffer solutions due to electron transfer from  $^3(4\text{-PyT})^*$  [or  $^3(\text{PuT})^*$ ] to  $MV^{2+}$ .

**Kinetics and Quantum Yield of Electron Transfer.** Each decay curve of  $^3(\text{PT})^*$  obeys first-order kinetics, giving the first-order rate constant ( $k_{\text{first}}$ ), which is in good agreement with the

**TABLE 1: Observed Rate Constants ( $k_{\text{obs}}$ ), Formation Quantum Yield ( $\Phi_{\text{et}}$ ) of  $\text{MV}^{\bullet+}$ , and Electron-Transfer Rate Constants ( $k_{\text{et}}$ ) for the Reaction between Triplet States of Thiones with  $\text{MV}^{2+}$  at 23 °C in Aqueous Buffer Solutions**

compd	pH	$k_{\text{obs}}^a$ ( $\text{M}^{-1} \text{s}^{-1}$ )	$\Phi_{\text{et}}^b$	$k_{\text{et}}^c$ ( $\text{M}^{-1} \text{s}^{-1}$ )
2-PyT	9.18	$2.7 \times 10^9$	0.55	$1.5 \times 10^9$
	7.00	$2.4 \times 10^9$	0.50	$1.2 \times 10^9$
	4.01	$2.2 \times 10^9$	0.45	$1.0 \times 10^9$
	1.68	$2.1 \times 10^9$	0.42	$8.8 \times 10^8$
4-PyT	9.18	$3.2 \times 10^9$	0.49	$1.6 \times 10^9$
	7.00	$3.1 \times 10^9$	0.42	$1.3 \times 10^9$
	4.01	$2.5 \times 10^9$	0.40	$1.0 \times 10^9$
	1.68	$2.4 \times 10^9$	0.39	$9.4 \times 10^8$
PuT	9.18	$3.3 \times 10^9$	0.43	$1.4 \times 10^9$
	7.00	$2.9 \times 10^9$	0.41	$1.2 \times 10^9$
	4.01	$2.7 \times 10^9$	0.38	$1.0 \times 10^9$
	1.68	$2.5 \times 10^9$	0.35	$8.7 \times 10^8$

<sup>a</sup> Estimation error is  $\pm 5\%$ . <sup>b</sup>  $\Phi_{\text{et}}$  was evaluated using eq 2 and from the plateau of the plot  $[\text{MV}^{\bullet+}]_{\text{max}}/[\text{}^3(\text{PT})^*]_{\text{max}}$  vs  $[\text{MV}^{2+}]$ ,<sup>20,21</sup> where  $\epsilon = 7140 \text{ M}^{-1} \text{ cm}^{-1}$  at 460 nm for  ${}^3(2\text{-PyT})^*$ ,  $6700 \text{ M}^{-1} \text{ cm}^{-1}$  at 430 nm for  ${}^3(4\text{-PyT})^*$ ,  $6100 \text{ M}^{-1} \text{ cm}^{-1}$  at 475 nm for  ${}^3(\text{PuT})^*$ , and  $1.37 \times 10^4 \text{ M}^{-1} \text{ cm}^{-1}$  at 600 nm for  $\text{MV}^{\bullet+}$  were used.<sup>13–15,19</sup> <sup>c</sup>  $k_{\text{et}} = \Phi_{\text{et}} k_{\text{obs}}$ .<sup>20,21</sup>

corresponding first-order rate constant evaluated from the rise curves of  $\text{MV}^{\bullet+}$  at 600 nm. These  $k_{\text{first}}$  values increase with  $[\text{MV}^{2+}]$ , giving the second-order rate constant ( $k_{\text{obs}}$ ) for  ${}^3(\text{PT})^*$  with  $\text{MV}^{2+}$  in aqueous solutions. They are summarized in Table 1.

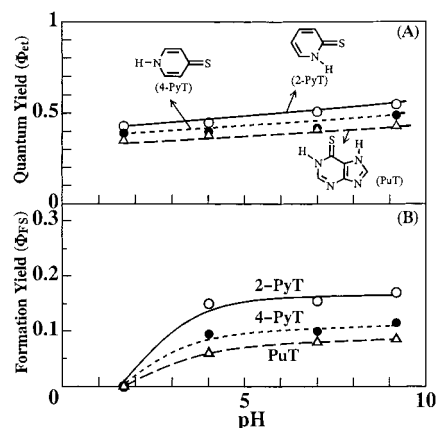
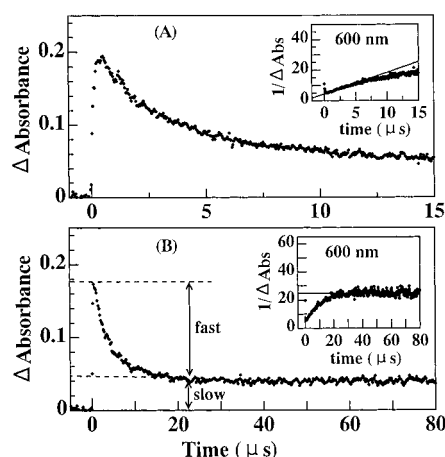
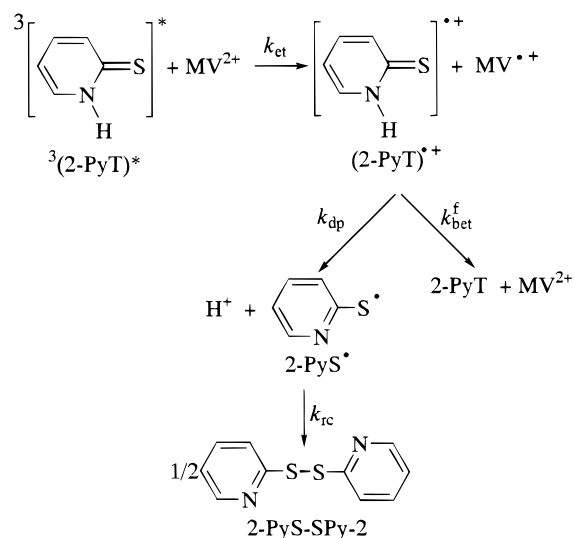
Since  ${}^3(\text{PT})^*$  and  $\text{MV}^{\bullet+}$  were observed in the same time frame, the efficiency of  $\text{MV}^{\bullet+}$  formation due to photoreduction of  $\text{MV}^{2+}$  via  ${}^3(\text{PT})^*$  could be calculated from the absorbance ( $A_{\text{C}}$  refers to maximum absorbance of  $\text{MV}^{\bullet+}$  and  $A_{\text{T}}$  to initial maximum absorbance of  ${}^3(\text{PT})^*$ ) and extinction coefficients ( $\epsilon_{\text{C}}$  refers to that of  $\text{MV}^{\bullet+}$  and  $\epsilon_{\text{T}}$  to that of  ${}^3(\text{PT})^*$ ) as in eq 2.<sup>20,21</sup>

$$[\text{MV}^{\bullet+}]_{\text{max}}/[\text{}^3(\text{PT})^*]_{\text{max}} = (A_{\text{C}}/\epsilon_{\text{C}})/(A_{\text{T}}/\epsilon_{\text{T}}) \quad (2)$$

Upon substitution of the reported values for  $\epsilon_{\text{C}}$  and  $\epsilon_{\text{T}}$ ,<sup>13–15,19</sup>  $[\text{MV}^{\bullet+}]_{\text{max}}/[\text{}^3(\text{PT})^*]_{\text{max}}$  values were evaluated. The plot of  $[\text{MV}^{\bullet+}]_{\text{max}}/[\text{}^3(\text{PT})^*]_{\text{max}}$  vs  $[\text{MV}^{2+}]$  reaches a plateau, yielding the electron-transfer quantum yield ( $\Phi_{\text{et}}$ ).<sup>20,21</sup> The  $\Phi_{\text{et}}$  values are listed in Table 1. All reaction systems in Table 1 show that  $\Phi_{\text{et}}$  values are in the range of ca. 0.40–0.55. This indicates that all of  ${}^3(\text{PT})^*$  was not always involved in the photoreduction of  $\text{MV}^{2+}$  to  $\text{MV}^{\bullet+}$ , suggesting that some deactivation processes such as charge-transfer interaction may take place concomitantly with the electron-transfer process. Thus, the rate constants ( $k_{\text{et}}$ ) for electron transfer from  ${}^3(\text{PT})^*$  to  $\text{MV}^{2+}$  can be evaluated by the relation  $k_{\text{et}} = \Phi_{\text{et}} k_{\text{obs}}$ .<sup>20,21</sup> These  $k_{\text{et}}$  values are also listed in Table 1. The values of  $\Phi_{\text{et}}$  and  $k_{\text{et}}$  are in the order 2-PyT > 4-PyT > PuT in each buffer solution, which may be related to the upper SOMO energies of triplet states of thiones. By MO calculations,<sup>17</sup> it was found that the higher the value of the upper SOMO energy of triplet states of thiones [ $-3.30 \text{ eV}$  for  ${}^3(2\text{-PyT})^*$ ,  $-3.32 \text{ eV}$  for  ${}^3(4\text{-PyT})^*$ , and  $-3.69 \text{ eV}$  for  ${}^3(\text{PuT})^*$ ], the higher is the value of  $\Phi_{\text{et}}$ ; i.e., the donor ability of  ${}^3\text{PT}^*$  increases with the high value of the upper SOMO energy.

The electron-transfer quantum yield ( $\Phi_{\text{et}}$ ) of  $\text{MV}^{\bullet+}$  for all PT/ $\text{MV}^{2+}$  systems at pH 9.18 is higher than those at pH 7.00 and 4.01 (Figure 5A), indicating that the formation of  $\text{MV}^{\bullet+}$  may be retarded with lowering pH. The values of  $k_{\text{et}}$  for all thiones at pH 9.18 are also larger than those at lower pH (Table 1).

**Back Electron Transfer.** In the transient measurements,  $\text{MV}^{\bullet+}$  begins to decay with two different time scales (fast and slow decay parts) after reaching a maximum, as shown in Figure 6. The fast decay part obeys second-order kinetics (inset in

**Figure 5.** Plots of (A) electron-transfer quantum yields ( $\Phi_{\text{et}}$ ) of  $\text{MV}^{\bullet+}$  vs pH obtained by transient absorption measurements and (B) steady-state formation yield ( $\Phi_{\text{SF}}$ ) of  $\text{MV}^{\bullet+}$  vs pH for the thione/ $\text{MV}^{2+}$  systems in aqueous buffer solutions.**Figure 6.** Absorption vs time profiles for the decay of  $\text{MV}^{\bullet+}$  at 600 nm within (A) 15  $\mu\text{s}$  and (B) 80  $\mu\text{s}$  obtained by laser photolysis of the 2-PyT/ $\text{MV}^{2+}$  system in aqueous solution at pH 7.00. The insets show second-order plots.**SCHEME 1****Figure 6.** which indicates that a part of  $\text{MV}^{\bullet+}$  reverts back to  $\text{MV}^{2+}$  by back electron transfer to  $\text{PyT}^{\bullet+}$  ( $k_{\text{bet}}^f$  in Scheme 1).  $k_{\text{bet}}^f$  was calculated from the slope ( $k_{\text{bet}}^f/\epsilon_{\text{MV}^{\bullet+}}$ ) of the second-order plot ( $1/\text{Abs}$  vs time) on substituting  $\epsilon_{\text{MV}^{\bullet+}} = 1.37 \times 10^4$

**TABLE 2: Percent Decays of  $MV^{•+}$  and Rate Constants for Back Electron Transfer Obtained from Both Fast and Slow Decay Parts of  $MV^{•+}$  by Transient Measurements and the Steady-State Formation Yield ( $\Phi_{SF}$ ) of  $MV^{•+}$  evaluated by Steady-Light Photolysis of Thione/ $MV^{2+}$  Systems at 23 °C in Aqueous Buffer Solutions<sup>a</sup>**

compd	pH	fast decay %	$k_{bet}^f$ <sup>b</sup> (M <sup>-1</sup> s <sup>-1</sup> )	slow decay %	$k_{bet}^s$ <sup>b</sup> (M <sup>-1</sup> s <sup>-1</sup> )	$\Phi_{SF}$ <sup>c</sup>
2-PyT	9.18	50.0	$5.0 \times 10^9$	50.0	$5.7 \times 10^5$	0.17
	7.00	74.2	$5.6 \times 10^9$	25.8	$5.6 \times 10^5$	0.16
	4.01	76.1	$5.5 \times 10^9$	23.9	$5.7 \times 10^5$	0.15
4-PyT	1.68	98.5	$5.6 \times 10^9$	~0.0	<i>d</i>	0.00
	9.18	65.3	$4.8 \times 10^9$	34.7	$6.6 \times 10^5$	0.12
	7.00	75.6	$5.0 \times 10^9$	24.4	$6.8 \times 10^5$	0.10
PuT	4.01	77.0	$5.3 \times 10^9$	23.0	$6.5 \times 10^5$	0.09
	1.68	99.1	$6.1 \times 10^9$	~0.0	<i>d</i>	0.00
	9.18	68.9	$4.4 \times 10^9$	31.1	$8.3 \times 10^5$	0.09
	7.00	74.9	$4.6 \times 10^9$	25.1	$8.3 \times 10^5$	0.08
	4.01	80.0	$4.8 \times 10^9$	20.0	$8.2 \times 10^5$	0.06
	1.68	98.9	$5.3 \times 10^9$	~0.0	<i>d</i>	0.00

<sup>a</sup> Estimation error is  $\pm 5\%$ . <sup>b</sup>  $k_{bet}^f$  and  $k_{bet}^s$  were evaluated from the second-order plots of the fast and slow decay parts of  $MV^{•+}$  at 600 nm, respectively, by using  $\epsilon = 1.37 \times 10^4 \text{ M}^{-1} \text{ cm}^{-1}$  for  $MV^{•+}$  at 600 nm.<sup>13,19</sup> <sup>c</sup>  $\Phi_{SF}$  was estimated by comparing the steady-state concentration (maximum) of  $MV^{•+}$  at 605 nm with the initial concentration of thiones (1.0 mM) in aqueous buffer solutions. <sup>d</sup> The long-lived  $MV^{•+}$  was not observed at pH 1.68.

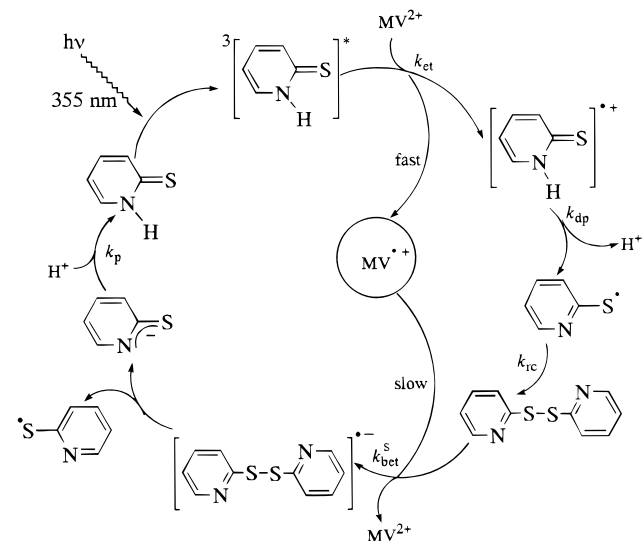
$\text{cm}^{-1} \text{ M}^{-1}$  at 600 nm.<sup>13,19</sup> The  $k_{bet}^f$  value is close to the diffusion-controlled limit,  $k_{diff} \approx \text{ca. } 6.4 \times 10^9 \text{ M}^{-1} \text{ s}^{-1}$ , in aqueous solutions.<sup>22</sup>

The slow decay part may correspond to the long-lived  $MV^{•+}$ .<sup>13,18,19</sup> The deprotonation reaction ( $k_{dp}$  in Scheme 1) of  $PyT^{•+}$  to the pyridylthio radical ( $PyS^{\bullet}$ ) may competitively occur with the back-electron-transfer reaction from  $MV^{•+}$  to  $PT^{•+}$ . Then,  $PyS^{\bullet}$  may recombine into disulfide ( $PyS-SPy$  in Scheme 1).<sup>16</sup> In the case of 2-PyT, 2-PyS<sup>•</sup> has an absorption maximum at 490 nm;<sup>16</sup> thus, a weak rise of the transient absorption band observed at 490 nm may be attributed to 2-PyS<sup>•</sup>, because of the low extinction coefficient of 2-PyS<sup>•</sup> ( $\epsilon \approx \text{ca. } 3000 \text{ M}^{-1} \text{ cm}^{-1}$  at 490 nm)<sup>16</sup> compared with  ${}^3(2-PyT)^*$  ( $\epsilon = 7140 \text{ M}^{-1} \text{ cm}^{-1}$  at 460 nm)<sup>15</sup> and  $MV^{•+}$  ( $\epsilon = 1.37 \times 10^4 \text{ M}^{-1} \text{ cm}^{-1}$  at 600 nm).<sup>13,19</sup> This observation supports the deprotonation of  $PyT^{•+}$  to  $PyS^{\bullet}$ .

From the long-decay time profile of  $MV^{•+}$  at 600 nm (Figure 6B), it was evaluated that 74.2% of the total of  $MV^{•+}$  follows the fast decay process and the rest (25.8%) follows the slow decay process in buffer solution at pH 7.00. This finding suggests that 74.2% of 2-PyT<sup>•+</sup> accepts an electron from  $MV^{•+}$ , while 25.8% of 2-PyT<sup>•+</sup> changes to 2-PyS<sup>•</sup>, which immediately converts to disulfide ( $k_{rc}$  in Scheme 1). Similarly, the percentages of the competitive decay processes for other systems in different buffer solutions were calculated as listed in Table 2, which shows that the formation efficiency of the long-lived  $MV^{•+}$  is higher (50.0% for 2-PyT/ $MV^{2+}$  system) at pH 9.18 than those at pH 7.00 and 4.01. It is natural that the deprotonation reaction of  $PyT^{•+}$  to  $PyS^{\bullet}$  may be easier at higher pH. The formation ability of the long-lived  $MV^{•+}$  for the 2-PyT/ $MV^{2+}$  system is higher than those for 4-PyT/ $MV^{2+}$  and PuT/ $MV^{2+}$  systems, which may be related to a higher deprotonation ability of 2-PyT<sup>•+</sup> than others.

The slow decay part also seems to obey second-order kinetics (inset in Figure 6), suggesting electron transfer from  $MV^{•+}$  to  $PyS-SPy$  (eq 3a), which may be slow because of an endothermic process. Such slow back electron transfer observed in this study is similar to the observations reported for aryl disulfides and distannanes.<sup>23,24</sup> The slope of the second-order plot of the slow decay part yielded  $k_{bet}^s = 5.6 \times 10^5 \text{ M}^{-1} \text{ s}^{-1}$  for the 2-PyT/ $MV^{2+}$  system due to electron transfer from  $MV^{•+}$

**SCHEME 2: Self-Repairing Cyclic Process for Photoreduction of  $MV^{2+}$  by  ${}^3(2-PyS)^*$  in Aqueous Solutions (pH > 4)**



to 2-PyS-SPy-2 in aqueous solution at pH 7.00 (Figure 6B). Similarly, the  $k_{bet}^s$  values for other systems in different buffer solutions were calculated as listed in Table 2.

The  $k_{bet}^s$  values are almost the same in all aqueous solutions (pH 9.18, 7.00, and 4.01), supporting the contribution of the disulfides, because the pH of the solution does not affect the properties of the disulfides. On the other hand, the values of  $k_{bet}^s$  decrease in the order  $PuT > 4-PyT > 2-PyT$ , which may be related to the electron-accepting ability of the corresponding disulfides. By MO calculations,<sup>17</sup> it was found that the lower the value of the LUMO energy of disulfide ( $-9.47 \text{ eV}$  for  $PuS-SPu$ ,  $-8.99 \text{ eV}$  for  $4-PyS-SPy-4$ , and  $-7.66 \text{ eV}$  for  $2-PyS-SPy-2$ ), the higher is the value of  $k_{bet}^s$  in aqueous solutions (Table 2). Since the LUMO of all the disulfides in our study has the  $\sigma^*$  character on the S-S bond, as pointed out by Shida,<sup>25</sup> the anion radicals of disulfides easily dissociate into the corresponding thio radicals and thiolate anions (eq 3b),<sup>23,24</sup> which accepts  $H^+$  returning to thione (eq 3c).



**Reaction Mechanism.** The whole reaction processes for the continuous photoreduction of  $MV^{2+}$  to generate  $MV^{•+}$  by 2-PyT as a representative of the thione photosensitizers can be illustrated as in Scheme 2. Since 2-PyS<sup>•</sup> produced by the dissociation of  $(2-PyS-SPy-2)^{\bullet-}$  can be reused to form  $(2-PyS-SPy-2)$  again, the whole process completely establishes a cycle, in which 2-PyT acts as a catalytic photosensitizer to produce  $MV^{•+}$ . It is noteworthy that thiones can repeatedly act as photosensitizer by their self-repairing ability to continuous reduction of  $MV^{2+}$  in aqueous solutions.

To identify the formation of disulfide as an intermediate of the photoinduced electron-transfer reactions between  $PT^*$ s and  $MV^{2+}$ ,  $O_2$  was added to the photoirradiated solutions containing maximal  $MV^{•+}$ .  $O_2$  accepts an electron from  $MV^{•+}$  leaving stable compounds, in which the disulfides were confirmed as described in the Experimental Section. This observation supports the radical coupling route of Scheme 1.



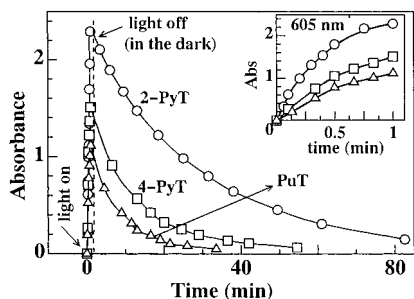


**Figure 7.** Plots of absorption intensity of  $MV^{\bullet+}$  at 605 nm vs time under steady light illumination and in the dark for thione/ $MV^{2+}$  systems in aqueous solution at pH 9.18. The inset shows the rise plots of  $MV^{\bullet+}$  at 605 nm.

The steady-state formation yield ( $\Phi_{SF}$ ) of  $MV^{\bullet+}$  was calculated by comparing the steady-state concentration (maximum) of  $MV^{\bullet+}$  at 605 nm with the initial concentration of thiones (1.0 mM), as listed in Table 2. The values of  $\Phi_{SF}$  did not change much in the pH range 4.01–9.18, as shown in Figure 5B, but drastically changed at pH values lower than ca. 4 and became zero at pH 1.68. This observation suggests that the deprotonation rate of thione radical cations is rather independent of pH in the range 4.01–9.18 but depends on pH values lower than ca. 4. In addition, this observation also suggests that the  $pK_a$  of thione radical cations may be within the range ca. 3–4. The fraction of the slow decay of  $MV^{\bullet+}$  has a close relation to  $\Phi_{SF}$  (Table 2). The decay rate of the steady-state concentration of  $MV^{\bullet+}$  after turning off the steady-illumination light increases in the order  $PuT > 4-PyT > 2-PyT$  (Figure 7), which is the same tendency as for  $k_{bet}^s$ . The rise rate of the steady concentration of  $MV^{\bullet+}$  during photoillumination increases in the order  $PuT < 4-PyT < 2-PyT$  (inset in Figure 7), which is the opposite tendency to the decay rates of a steady concentration of  $MV^{\bullet+}$ . Thus, it is clearly indicated that the rate-determining step is the one electron-reduction of disulfide by  $MV^{\bullet+}$  in the aqueous solutions.

**In Strong Acidic Solution.** At pH 1.68, no spectral change for the generation of the long-lived  $MV^{\bullet+}$  was observed by steady-light illumination of thione/ $MV^{2+}$  systems. The transient measurements afforded the evidence for photoinduced electron transfer from  ${}^3(PT)^*$  to  $MV^{2+}$ , forming  $MV^{\bullet+}$  at 600 nm even in buffer solution at pH 1.68 with  $k_{et}$  similar to those at higher pH; the strong acidic solution may cause only a slight decrease in  $k_{et}$ . The  $k_{bet}$  values in strong acidic solution are also similar to  $k_{bet}^f$  values at higher pH (Table 2). Thus,  $\Phi_{SF} = 0$  in strong acidic solution may be attributed to the absence of a slow decay component of the  $MV^{\bullet+}$ , which indicates that  $PT^{\bullet+}$  has a longer lifetime, probably because the deprotonation of  $PT^{\bullet+}$  is retarded in a strong acid; the high fraction (almost 100%) of quick back electron transfer from  $MV^{\bullet+}$  to  $PT^{\bullet+}$  causes the short-lived  $MV^{\bullet+}$  at pH 1.68.

## Conclusions

The long-lived  $MV^{\bullet+}$  was observed by the photoexcitation of PT in the presence of  $MV^{2+}$ . The reaction mechanism was revealed by the combination of steady-state photolysis with laser flash photolysis. It was shown that electron-transfer-induced photoreduction of  $MV^{2+}$  to  $MV^{\bullet+}$  has been sensitized by  ${}^3(PT)^*$

in aqueous buffer solutions. The long-lived  $MV^{\bullet+}$  was caused by deprotonation of  $PT^{\bullet+}$ , which occurs competitively with back electron transfer from  $MV^{\bullet+}$  to  $PT^{\bullet+}$ . The reproducibility for the production of the long-lived  $MV^{\bullet+}$  indicates that deprotonation of  $PT^{\bullet+}$  yields the thio radical, which is immediately converted into disulfide with less efficient electron-accepting ability by a radical coupling reaction. The slow oxidation of  $MV^{\bullet+}$  to  $MV^{2+}$  was assigned to endothermic electron transfer to the disulfide. Finally, thione was recovered by reprotonation of thiolate anion, which is produced by disproportionation of the radical anion of disulfide. These processes are quite reproducible, suggesting that 2-PyT, 4-PyT, and PuT are quite efficient photosensitizers having self-repairing ability for the continuous photoreduction of  $MV^{2+}$  without using a sacrificial electron donor.

## References and Notes

- (1) Bard, A. J.; Ledwith; Shine, H. J. *Adv. Phys. Org. Chem.* **1976**, *13*, 155.
- (2) Anderson, R. F. Z. *Phys. Chem.* **1976**, *80*, 969.
- (3) Bocarsley, A. B.; Bookbinder, D. C.; et al. *J. Am. Chem. Soc.* **1980**, *102*, 368.
- (4) Bard, A. J.; Bocarsley, A. B.; et al. *J. Am. Chem. Soc.* **1980**, *102*, 3671.
- (5) Bird, C. L.; Kuhn, A. T. *Chem. Soc. Rev.* **1981**, *10*, 49.
- (6) Harriman, A.; Mills, A. J. *Chem. Soc., Faraday Trans. 2* **1981**, *77*, 2111.
- (7) (a) Mandal, K.; Hoffman, M. Z. *J. Phys. Chem.* **1984**, *88*, 185. (b) Feilchenfeld, H.; Chumanov, G.; Cotton, T. M. *J. Phys. Chem.* **1996**, *100*, 4937.
- (8) Nenadovic, M. T.; Micic, O. I.; Adzic, R. R. *J. Chem. Soc., Faraday Trans. 1* **1982**, *78*, 1065.
- (9) (a) Nenadovic, M. T.; Micic, O. I.; Rajh, T.; Savic, D. *J. Photochem.* **1983**, *21*, 35. (b) Kasuga, K.; Miyasaka, H.; Handa, M.; Dairaku, M. *Polyhedron* **1995**, *14*, 1675.
- (10) (a) Szulbinski, W. S. *Inorg. Chim. Acta* **1998**, *269*, 253. (b) Smith, P. R.; Holmes, J. D.; Richardson, D. J.; Russell, D. A.; Sodeau, J. R. *J. Chem. Soc., Faraday Trans.* **1998**, *94*, 1235. (c) Song, X.-Z.; Jia, S.-L.; Miura, M.; Ma, J.-G.; Shelnut, J. A. *J. Photochem. Photobiol. A* **1998**, *113*, 233.
- (11) Prasad, D. R.; Hoffman, M. Z.; Mulazzani, Q. G.; Rodgers, M. A. *J. Am. Chem. Soc.* **1986**, *108*, 5135.
- (12) Georgopolous, M.; Hoffman, M. Z. *J. Phys. Chem.* **1991**, *95*, 7717.
- (13) Kim, Y.-S.; McNiven, S.; Ikebukuro, K.; Karube, I. *Photochem. Photobiol.* **1997**, *66*, 180.
- (14) Alam, M. M.; Fujitsuka, M.; Watanabe, A.; Ito, O. *J. Phys. Chem. A* **1998**, *102*, 1338.
- (15) Alam, M. M.; Fujitsuka, M.; Watanabe, A.; Ito, O. *J. Chem. Soc., Perkin Trans. 2* **1998**, 817.
- (16) (a) Alam, M. M.; Watanabe, A.; Ito, O. *J. Org. Chem.* **1995**, *60*, 3440. (b) Alam, M. M.; Watanabe, A.; Ito, O. *Photochem. Photobiol.* **1996**, *63*, 53. (c) Ha, C.; Horner, J. H.; Newcomb, M.; Varick, T. R.; Arnold, B. R.; Luszyk, J. *J. Org. Chem.* **1993**, *58*, 1194.
- (17) (a) Dewar, M. J. S.; et al. *J. Am. Chem. Soc.* **1985**, *107*, 3902. (b) Stewart, J. J. P. *J. Comput. Chem.* **1989**, *10*, 209.
- (18) (a) Takuma, K.; Kajiwara, M.; Matsuo, T. *Chem. Lett.* **1977**, 1199. (b) Kalyanasundaram, K.; Dung, D. *J. Phys. Chem.* **1980**, *84*, 2402.
- (19) Watanabe, T.; Honda, K. *J. Phys. Chem.* **1982**, *86*, 2617.
- (20) (a) Alam, M. M.; Watanabe, A.; Ito, O. *J. Photochem. Photobiol. A* **1997**, *104*, 59. (b) Alam, M. M.; Watanabe, A.; Ito, O. *Bull. Chem. Soc. Jpn.* **1997**, *70*, 1833.
- (21) Alam, M. M.; Sato, M.; Watanabe, A.; Akasaka, T.; Ito, O. *J. Phys. Chem. A* **1998**, *102*, 7447.
- (22) Calvert, J. G.; Pitts, J. N., Jr. *Photochemistry*; John Wiley & Sons: New York, 1966; pp 626–627.
- (23) Tagaya, H.; Aruga, T.; Ito, O.; Matsuda, M. *J. Am. Chem. Soc.* **1981**, *103*, 5484.
- (24) Aruga, T.; Ito, O.; Matsuda, M. *J. Phys. Chem.* **1982**, *86*, 2950.
- (25) Shida, T. *J. Phys. Chem.* **1968**, *72*, 2597.